Calmodulin-Sensitive Interaction of Human Nebulin Fragments with Actin and Myosin†

Douglas D. Root and Kuan Wang*

Department of Chemistry and Biochemistry, The Biochemical Institute and Cell Research Institute, University of Texas at Austin, Austin, Texas 78712

Received June 9, 1994; Revised Manuscript Received July 25, 1994®

ABSTRACT: Nebulin is a giant protein ruler of the actin filament of skeletal muscle. This modular protein primarily consists of a repeating sequence (module) of 35 residues and a superrepeat of seven modules. These modules are thought to be actin binding domains along the length of nebulin. Cloned human nebulin fragments of 7–8 modules bind with high affinity to calmodulin, actin, myosin, and myosin head. The stoichiometry of high-affinity binding is approximately one actin monomer bound per nebulin fragment and one myosin bound per nebulin fragment, as determined by cosedimentation binding assays. These observations raise the intriguing possibility that nebulin might have regulatory functions on actomyosin interactions. Nebulin fragments from the N-terminal half situated in the actomyosin overlap region of the sarcomere inhibit actomyosin ATPase activity and the sliding velocity of actin over myosin in motility assays, while a nebulin fragment near the C-terminus, which is localized to the Z-line, does not prevent actin sliding. Calmodulin reverses the inhibition of ATPase and accelerates actin sliding in a calcium-dependent manner. Calmodulin with calcium greatly reduces the binding of nebulin fragments to both actin and myosin. The data suggest that the nebulin can interact with both actin and myosin in a calcium/calmodulin-dependent manner and might have regulatory functions in skeletal muscle contraction in a fashion analogous to caldesmon in smooth muscle.

Nebulin, a large protein of skeletal muscle (600–900 kDa), has been proposed to be a length-regulating template for actin in the thin filament (Wang, 1985; Wang & Wright, 1988; Pierobon-Bormioli et al., 1989; Maruyama et al., 1989; Labeit et al., 1991). This modular protein primarily consists of a repeating sequence (module) of 35 residues and a superrepeat of seven modules (Stedman et al., 1988; Wang et al., 1990; Jin & Wang, 1991a; Labeit et al., 1991). These modules are thought to be actin binding domains along the length of nebulin (Jin & Wang, 1991a,b; Kruger et al., 1991; Chen et al., 1993). Since a single nebulin molecule coextends with actin filaments in the sarcomere with the C-terminus anchored at the Z-line (Kruger et al., 1991; Wright et al., 1993), nebulin is likely to be a very elongated protein (~1 μm) with multiple binding sites that forms a zipper-like composite thin filament (Chen et al., 1993; Chen & Wang, 1994; Pfuhl et al., 1994). Nebulin's lateral association with actin and its seven-module superrepeating structure suggest some structural parallels with the troponin–tropomyosin system on the thin filaments. A single tropomyosin and troponin complex binds seven actin monomers and acts as a calcium-regulated switch along the actin filament. It is thought that the signal induced by calcium binding to troponin C is transmitted cooperatively along the actin filament to the seven actin molecules. This calcium-mediated switch can turn on and off both actomyosin ATPase and actin sliding over myosin *in vitro* [for a review, see Zot and Potter (1987)]. A distinct calcium regulatory system also operates via myosin. It has been proposed that the amount of force generated during the isometric contraction of a muscle can be potentiated through phosphorylation by the calmodulin-requiring myosin light-chain kinase (Sweeney et al., 1993). Thus, there are two complementary calcium regulatory pathways that are currently known in skeletal muscle.

In smooth muscle, there are three systems capable of calcium-mediated regulation of actomyosin interactions *in vitro*: myosin light-chain kinase, caldesmon, and calponin [for a review, see Walsh (1990)]. Caldesmon and calponin bind both actin and myosin, which has made them likely candidates for the regulation of smooth muscle. In conjunction with calcium/calmodulin and/or phosphorylation, these proteins are capable of switching on and off actomyosin ATPase and actin sliding over myosin *in vitro* (Shirinsky et al., 1992). The existence of multiple regulatory systems in smooth muscle raises the question of whether skeletal muscle might also have additional regulatory systems and, in particular, whether nebulin might be a candidate.

Because of technical difficulties in purifying native nebulin, the functional characteristics of this protein have only recently begun to be investigated. The preparation of cloned fragments of nebulin has greatly facilitated the functional characterization of this large protein (Jin & Wang, 1991a,b; Kruger et al., 1991; Chen et al., 1993). Cloned nebulin fragments of 7–8 modules that are localized to the thin and thick filament overlap region of the sarcomere bind to both actin and myosin (Jin & Wang, 1991a,b; Kruger et al., 1991). These observations raised the intriguing possibility that nebulin might have regulatory functions on actomyosin interactions (Jin & Wang, 1991a). We explored this idea by characterizing the binding of the fragments to actin and myosin and examining their effects on actomyosin ATPase activity and the sliding velocity of actin over myosin during *in vitro* motility assays. Our data provide strong support for thin-filament-based regulatory functions of nebulin in skeletal muscle.

† D.R. was supported by a postdoctoral fellowship from the Muscular Dystrophy Association of America. This work is supported by grants from the NIH (DK20270 to K.W.) and the Foundation for Research (to K.W.).

* Address correspondence to this author at the Department of Chemistry and Biochemistry, Welch 4.230C, The University of Texas at Austin, Austin, TX 78712. Telephone: 512-471-4065. Fax: 512-471-4065.

® Abstract published in *Advance ACS Abstracts,* September 1, 1994.

0006-2960/94/0433-12581$04.50/0

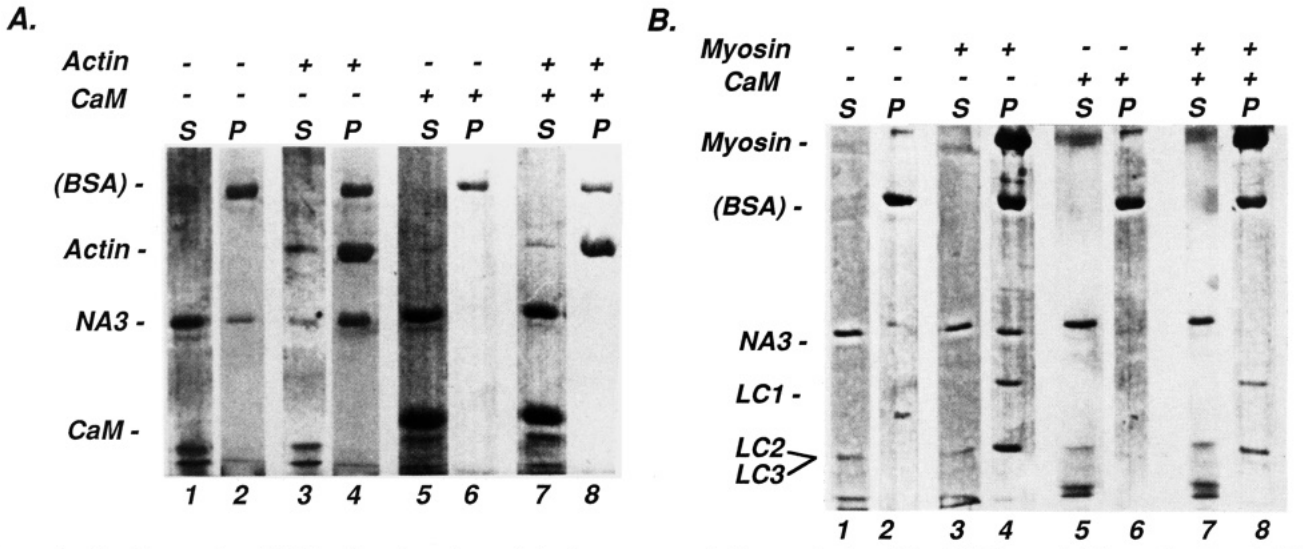

FIGURE 1: Cosedimentation of NA3 with actin and myosin in the presence and absence of calmodulin. NA3 (up to 6 μM) was incubated with fixed concentrations of actin (0.95 μM) or myosin (3.3 μM), either in the presence (+) or absence (–) of calmodulin (6 μM CaM) in 25 mM KCl, 4 mM $MgCl_2$, 1 mM $CaCl_2$, and 10 mM imidazole (pH 7.0). After sedimentation, supernatants (S) and pellets (P) were analyzed by SDS–PAGE. To facilitate quantitation, bovine serum albumin (BSA) was added to unwashed pellets to normalize recovery. (A) NA3 (0.3 μM)–actin (0.95 μM) binding. Coomassie Blue-stained gel patterns. (B) NA3 (0.3 μM)–myosin (0.05 μM) binding. Silver-stained gel patterns. LC1, LC2, and LC3: Myosin light chains.

EXPERIMENTAL PROCEDURES

Proteins. Rabbit skeletal actin was prepared by the method of Spudich and Watt (1971). Rabbit skeletal myosin and α-chymotryptic myosin subfragment-1 (S-1)[1] or heavy meromyosin (HMM) were prepared by the method of Godfrey and Harrington (1970). The cloned human nebulin fragments were purified as described (Jin & Wang, 1991a,b), except that isolated inclusion bodies were dissolved in 6 M urea, 1 mM EDTA, and 10 mM imidazole (pH 7.0), separated on a CM52 ion-exchange column equilibrated in the same buffer, and eluted with a 0–0.5 M NaCl gradient. The resulting fractions were dialyzed against 1 mM $CaCl_2$ and 10 mM imidazole (pH 7.0) and centrifuged at 100000*g* to remove aggregates prior to use. Dialysis to near millimolar concentrations of calcium was found to increase the solubility of nebulin fragments in the absence of urea from about 0.7 to 6 μM for NA4 and from 2 to 18 μM for NA3. Porcine brain calmodulin was procured from Sigma (St. Louis, MO). Rabbit skeletal troponin and tropomyosin were prepared as described (Smillie, 1982; Potter, 1982).

Protein concentrations were determined spectrophotometrically. The following extinction coefficients ($A^{1\%}_{280nm}$) and molecular weights, respectively, were used: myosin, 5.5 cm^{-1}, 500 000 (Godfrey & Harrington, 1970); HMM, 6.5 cm^{-1}, 350 000 (Young et al., 1965); S-1, 7.5 cm^{-1}, 110 000 (Weeds & Pope, 1977); actin, 11.0 cm^{-1}, 42 000 (West et al., 1967); troponin, 4.5 cm^{-1}, 69 000 (Eisenberg & Kielley, 1974); tropomyosin, 3.3 cm^{-1}, 66 000 (Cummins & Perry, 1973). The extinction coefficients ($A^{1\%}_{280nm}$) calculated according to Gill and von Hippel (1989) of cloned nebulin fragments and their molecular weights were as follows: NA3, 13.2 cm^{-1}, 31 419; NA4, 13.4 cm^{-1}, 27 945; NC17, 17.8 cm^{-1}, 28 568.

[1] Abbreviations: BCIP/NPT, bromochloroindolyl phosphate/nitro blue tetrazolium; CaM, calmodulin; ELISA, enzyme-linked immunosorbent assay; HMM, heavy meromyosin; ISIT, intensified silicon-intensified target; NA3, NA4, NC17, ND8, and ND66, cloned nebulin fragments; PAGE, polyacrylamide gel electrophoresis; rpm, rotations per minute; r^2, correlation coefficient; SD, standard deviation; SDS–PAGE, sodium dodecyl sulfate–polyacrylamide gel electrophoresis; SE, standard error of the mean; S-1, myosin subfragment-1; LC1, LC2, and LC3, myosin light chains; TBS, Tris-buffered saline.

Cosedimentation Binding Assays. Cosedimentation assays typically were performed by incubating varying concentrations of nebulin fragments (up to 7 μM) with fixed concentrations of actin (0.95 μM) or myosin (3.3 μM) and spinning for 2 h at 35 000 rpm in a Beckman L5-50 ultracentrifuge at 20 °C. The supernatants were removed, and the pellets, without washing, were solubilized overnight at 4 °C in a fixed volume of 6 M urea, 10 mM imidazole (pH 7.0), and 0.1 mg/mL bovine serum albumin (BSA) as an internal standard to control for dilution and protein recovery. The proteins in the pellets and supernatants were separated by SDS–PAGE (12%; Laemmli, 1970), stained by Coomassie Blue or silver (Gotlieb & Chavoko, 1987), and compared to standard curves of nebulin fragments, actin, and bovine serum albumin. Densitometry of the stained gels was performed by a flatbed scanner system previously described (Root & Wang, 1993). Less than 10% of the total nebulin fragment pelleted and/or adsorbed to the centrifuge tube walls in the absence of actin or myosin (e.g., Figure 1A, lane 2). The concentration of unpelleted actin was determined from the supernatants, and this value was subtracted from the total actin. The binding data were analyzed by a model that assumes one class of independent binding sites for the reaction:

$$B \overset{K_d}{\rightleftharpoons} A + F$$

The equation for nonlinear curve fitting (by Curve Fit, K. Raner, 1991) is

$$B = [nP + K_d + N - \sqrt{(nP + K_d + N)^2 - 4nPN}]/2$$

where B is the molar concentration of bound nebulin fragments, n is the number of independent nebulin binding sites per mole of P, P is the total molar concentration of actin or myosin, N is the total molar concentration of NA3 or NA4, K_d is the microscopic (site) dissociation constant ($=(N-B)(nP-N)/B$), A is the molar concentration of free nebulin binding sites on P ($=nP-B$), and F is the molar concentration of free NA3 or NA4.

The dependent variable was chosen as the total protein concentration that was varied, since this is measured more

precisely than the calculated free concentration and thus is more suitable for numerical analysis.

Solid-Phase Binding Assays. Microtiter plate assays were performed by first coating plates with 0.1 mL of 1.5 μM NA3 or 2.0 μM calmodulin overnight at 4 °C in 1 mM $CaCl_2$ and 10 mM imidazole (pH 7.0), followed by washing three times with TBS blocking buffer (150 mM NaCl, 0.05% Tween-20, 0.2% BSA, and 10 mM Tris, pH 7.4). The amount of NA3 or calmodulin adsorbed was determined by copper staining on a duplicate plate (Root & Reisler, 1990). The plates were blocked with the TBS blocking buffer for 1 h at 37 °C. Incubations with actin (0–4.9 μM) or myosin (0–1.3 μM) were done at 20 °C for 1 h. Mouse monoclonal antibodies N107 against NA3, F59 against S-1 (Miller et al., 1989), or JLA20 against actin (Lin, 1981) and peroxidase-conjugated secondary antibodies were each incubated for 1 h at 37 °C in the TBS blocking buffer, with three washing steps in between. Color development of 2,2′-azinobis(3-ethylbenzthiazoline-6-sulfonic acid) was monitored at 405 nm at 4 min intervals with an EIA reader (BioTek Instruments Inc., Burlington, VT), and the rates were determined by linear curve fitting ($r^2 > 0.95$). Background rates were subtracted out. For dot-blot assays, 10 μL aliquots of F-actin (3 μM) or S-1 (3 μM) were dotted on a nitrocellulose membrane and allowed to dry. The membrane was blocked in TBS blocking buffer and then incubated with NA4 (0.3 μM) in TBS blocking buffer for 1 h at 20 °C. The bound NA4 was detected by the monoclonal antibody against NA4 and alkaline phosphatase-conjugated goat anti-mouse secondary antibody developed with BCIP/NPT.

ATPase Assays. The calcium ATPases were measured in 50 mM KCl, 5 mM $CaCl_2$, and 2 mM Tris (pH 7.4) (Kielley & Bradley, 1956). The magnesium ATPases were measured in 4 mM $MgCl_2$, 1 mM $CaCl_2$, and 25 mM imidazole (pH 7.0), plus 25 mM KCl for myosin or 2 mM KCl for S-1 (Root & Reisler, 1992). Actin-activated ATPase activities were assayed with 1 μM actin, and the basal magnesium ATPase activity was subtracted out. The phosphate released from ATP (2 mM) at 25 °C was determined by the malachite green assay (Baykov et al., 1988).

Motility Assays. The sliding velocities of rhodamine phalloidin-labeled actin over α-chymotryptic heavy meromyosin on a nitrocellulose-coated coverslip (Kron et al., 1991; Homsher et al., 1992) were observed at 20 °C with an ISIT (Dage 66) mounted on a Zeiss Universal fluorescence microscope and recorded with an SVHS video recorder (JVC, HR-S8000U). Frames were averaged and grabbed for analysis with Image 1.47 (Wayne Rasband, NIH). An in-house macro for Image, TRACK1.47, was developed to determine the actin sliding velocities from the contour lengths of tracks of moving filaments. Only filaments that moved continuously for at least 6 s and 20 frames were analyzed. Each leading edge plot represents the sum of 23 binary images grabbed at 3 frames/s, from which the first frame is subtracted. The assay buffer contained 25 mM KCl, 4 mM $MgCl_2$, 0.1 mM $CaCl_2$, 1 mM ATP, 10 mM dithiothreitol, 25 mM imidazole (pH 7.0), 0.5% methylcellulose, 3 mg/mL glucose, 0.1 mg/mL catalase, and 0.1 mg/mL glucose oxidase (Kron et al., 1991). The assay buffer was supplemented with EGTA up to 0.4 mM for calcium dependence experiments. The free calcium concentration was calculated with the program SPECS, developed by Fabiato (1988). Test measurements were compared to control values from the same coverslip.

Table 1: Dissociation Constants from Cosedimentation Assays[a]

proteins	dissociation constant K_d (μM)	stoichiometry (n)	r^2
NA3 and actin	0.9 ± 0.2	1.6 ± 0.1	0.990
NA4 and actin	0.13 ± 0.05	0.95 ± 0.06	0.983
NA3 and myosin	0.16 ± 0.05	1.10 ± 0.12	0.949

[a] The cosedimentation binding assays were performed as described for Figure 1. Errors indicate standard error of the mean.

RESULTS

The interactions of nebulin fragments with actin and myosin were characterized by four types of assays: (1) cosedimentation assays of nebulin fragments with F-actin and synthetic myosin filaments; (2) ELISA with specific monoclonal antibodies to detect the binding of actin and myosin head to adsorbed nebulin fragments on microtiter plates; (3) calcium-, magnesium-, and actin-activated ATPase assays of myosin and S-1 in the presence of nebulin fragments; and (4) *in vitro* motility assays to test the effect of nebulin fragments on the actin sliding velocity over myosin. As part of our search for potential regulatory mechanisms of these interactions, experiments were also carried out in the presence of calmodulin and calcium. Of the human nebulin molecule, a total of 128 kDa has been bacterially expressed as protein fragments. Three fragments, NA3, NA4, and NC17, each containing 7–8 modules, are from the N-terminal side of nebulin, which is normally located in the overlap region of the sarcomere. Two additional fragments ND8 (2 modules) and ND66 (4 modules) have been cloned from the C-terminus, which is located at or near the Z-line region. We have previously reported that the interaction of ND8 with actin affects actin polymerization (Chen et al., 1993). In the present study, emphasis is placed on the characterization of nebulin fragments from the overlap region. An improvement in the solubility of these fragments (by incorporating Ca^{2+} during dialysis) allows protein interactions to be studied with a broader range of techniques. Two fragments, NA4 and NA3, are studied and reported in detail; other fragments gave similar qualitative results.

Binding of Nebulin Fragments to Actin, Myosin, S-1, and Calmodulin. Cosedimentation of F-actin with NA3 in 25 mM KCl, 4 mM $MgCl_2$, 1 mM $CaCl_2$, and 10 mM imidazole (pH 7.0) was done by varying the NA3 concentrations at a fixed F-actin concentration (0.95 μM). As shown in Figure 1A, soluble NA3 (lanes 1 and 2) was brought down by F-actin (lanes 3 and 4). Quantitative analysis of gel patterns indicated that the binding curve (Figure 2C) is well fit by assuming a simple class of binding sites with a K_d of 0.9 ± 0.2 μM and a stoichiometry (n) of 1.6 ± 0.1 (SE) mol of NA3 monomer per actin protomer (Table 1). Parallel studies with NA4 gave similar results: K_d = 0.13 ± 0.05 μM and n = 0.95 ± 0.06 (Table 1). These stoichiometric values are well below the expected n = 8 for NA3 and n = 7 for NA4, if each module binds one actin protomer with the same affinity (Chen et al., 1993). Instead, these data indicate that there is one or no more than two high-affinity (submicromolar) actin binding sites per nebulin superrepeat under the conditions of these experiments (see Discussion).

The dissociation constant was also obtained from the quantitative solid-phase binding assays (ELISA, Figure 2A). NA3 was adsorbed on a microtiter plate, and the amount of NA3 coated per well (6.5 ± 0.3 ng (SE)) was determined by copper staining (Root & Reisler, 1990). Because the amount of actin that could be bound by this low concentration of NA3 was much less than the total actin concentrations that were

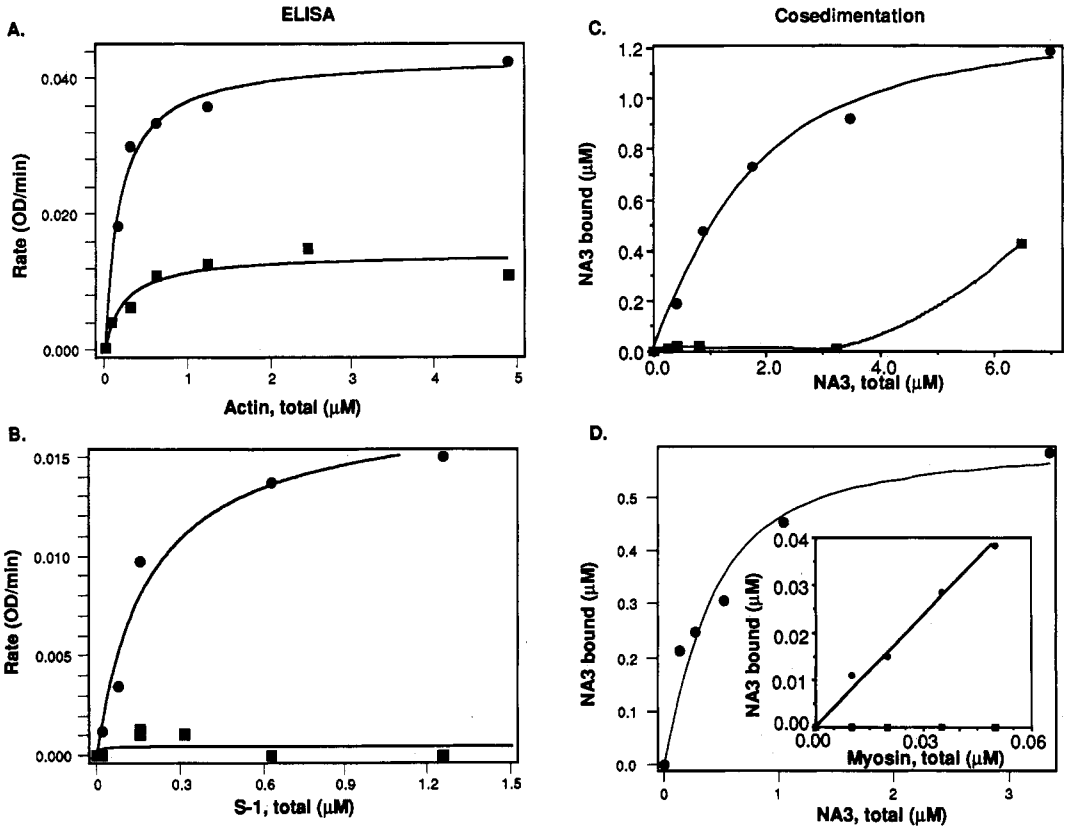

FIGURE 2: Calcium–calmodulin-sensitive binding of NA3 to actin and myosin. The binding of nebulin fragment NA3 to actin in the presence (■) and absence (●) of 6 μM calmodulin and 1 mM calcium was measured by ELISA (A and B) and by cosedimentation assays (C and D). The buffer conditions were the same as for Figure 1. (A) The binding curves of F-actin (0.16–2.5 μM) to adsorbed NA3 as determined by ELISA. (B) The binding curves of S-1 (0.04–1.25 μM) to adsorbed NA3 as measured by ELISA. (C) The binding curves of NA3 to F-actin as determined by cosedimentation of actin (0.95 μM) with varying concentrations of NA3 (0.4–7.0 μM), as for Figure 1. The concentration value of unpelleted actin, 0.13 μM, was subtracted from the value for total actin. For each concentration of NA3, background NA3 in the absence of actin was subtracted out. (D) The binding curves of varying concentrations of NA3 (0.13–3.35 μM) to myosin (0.276 μM) as measured by cosedimentation assays. The conditions were as for Figure 1. For each concentration of NA3, background NA3 in the absence of myosin was subtracted out. Inset: The binding curves of varying concentrations of myosin (0.01–0.05 μM) to NA3 (0.3 μM) in the presence (■) and absence (●) of 6 μM calmodulin and 1 mM calcium, as measured by cosedimentation assays. All curves in the absence of calmodulin were calculated using a one-class binding model. Except for A and B, all curves in the presence of calmodulin were fit by interpolation.

used, the free and total actin concentrations were assumed to be equal for curve-fitting purposes. The relative amount of bound actin was estimated by the linear rate of peroxidase activity from a horseradish peroxidase-conjugated secondary antibody. The following Michaelis–Menten-like hyperbolic equation was derived to fit the data:

$$R = R_m P/(K_d + P)$$

where R is the rate of the enzyme reaction, P is the total actin concentration, K_d is the microscopic dissociation constant, and R_m is the maximum peroxidase rate at saturation. Because ELISA measures the relative degree of binding and not the absolute amount of actin bound, the stoichiometry of the interaction cannot be determined. A comparison of the dissociation constants from the ELISA and cosedimentation assay data provides validation of the ELISA as a method for determining the binding constant. The estimated dissociation constant of actin binding to solid-phase NA3 was 0.11 ± 0.04 μM (SE). This value is comparable in magnitude to that determined from cosedimentation (0.9 ± 0.2 μM, Table 1). Therefore, apparent dissociation constants of actin to NA3 either in solution or on the solid phase are submicromolar. The binding of nebulin fragment NA4 to actin is similar (Table 1).

The binding of NA3 to actin was shown to be sensitive to the presence of calmodulin and calcium (Figures 1A and 2A,C). The presence of calmodulin and calcium did not completely block the binding of NA3 to actin (Figure 2A,C), but it did largely reduce the amount of binding. Control ELISA experiments were done by binding actin to adsorbed NA3 in the presence of 10 mM EGTA and the presence (K_d = 0.16 ± 0.06 μM, r^2 = 0.937) or absence (K_d = 0.20 ± 0.03 μM, r^2 = 0.991) of calmodulin. The binding profiles were indistinguishable from those in the presence of calcium and without calmodulin.

NA3 bound tightly to adsorbed calmodulin as determined by ELISA (Figure 3). There was no detectable difference in the binding profiles of NA3 to calmodulin in the presence or absence of 10 mM EGTA to chelate calcium (Figure 3). The data indicate that calmodulin induces a calcium-sensitive conformational change in NA3 that modulates its binding to actin. The estimated dissociation constant from the combined data set was 0.60 ± 0.15 μM (SE, r^2 = 0.832).

The interaction of NA3 with myosin was established by cosedimentation assays with synthetic myosin filaments in solution. The cosedimentation of various concentrations of myosin with fixed concentrations of NA3 (Figure 2D) gave a binding curve that was well fit by a model assuming one class of independent binding sites: a binding stoichiometry of 1.10 ± 0.12 (SE) mol of NA3 per double-headed myosin and a dissociation constant of 0.18 ± 0.05 μM (Table 1). Thus, NA3 bound myosin more tightly than actin in cosedimentation assays. Parallel experiments with chymotryptic myosin rods

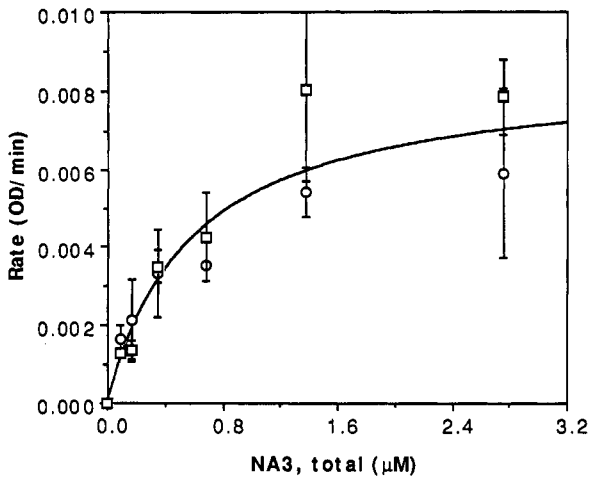

FIGURE 3: Binding of NA3 to calmodulin. Various concentrations of NA3 (0.09–2.75 μM) were incubated with solid-phase calmodulin (<0.1 μM) in microtiter plates in the presence of Ca (○, in the same buffer as for Figure 1) and in the absence of Ca (□, 10 mM EGTA). The curve was calculated from the combined data set to a simple binding model. Error bars indicate the standard error of the mean of triplicate determinations.

showed no cosedimentation with NA3 (not shown), indicating that NA3 most likely binds to myosin heads.

The interaction of NA3 with myosin heads was verified by studying the binding of subfragment-1 (S-1) to NA3 that was absorbed on the microtiter plate (Figure 2B). The binding curve yielded a K_d of 0.19 ± 0.06 μM (SE, $r^2 = 0.970$), which agrees well with the dissociation constant of NA3-intact myosin complexes estimated from cosedimentation assays of NA3 and intact myosin (Table 1). The stoichiometry, however, cannot be determined from the ELISA, because only relative amounts of bound S-1 are measured.

The binding of NA4 to S-1 was demonstrated qualitatively by dot-blotting assays on nitrocellulose paper. S-1 and actin were applied in equal molar amounts (1.0 pmol/mm^2) to nitrocellulose paper, which was subsequently blocked by BSA and incubated with 0.3 μM NA4. The bound NA4 was detected by a monoclonal antibody specific for NA4 and an alkaline phosphatase-conjugated secondary antibody. The binding of NA4 to S-1 was 6-fold stronger than binding to the same molar amount of F-actin on nitrocellulose (not shown).

Interestingly, the presence of calmodulin with calcium also inhibited the binding of NA3 to myosin and S-1 (Figure 2B,D, inset). Control ELISA experiments with the binding of S-1 to adsorbed NA3 in the presence of 10 mM EGTA yielded binding profiles that were unaffected by the presence or absence of calmodulin and indistinguishable from binding isotherms in the presence of calcium alone.

Effect of Nebulin Fragments on ATPase Activity. The binding of NA3 and NA4 to actin and myosin led us to investigate their effects on the ATPase activities of myosin and S-1, either alone or in the presence of actin (Figures 4–6). It was observed that these fragments (2 μM NA3 and 1 μM NA4) marginally accelerated the calcium and magnesium ATPase activities of myosin (0.25 μM) and S-1 (0.5 μM) in the absence of actin (Figure 4). Of this data set, only the NA4 activations of S-1 calcium ATPase and myosin magnesium ATPase activities were statistically significant. In contrast, the actomyosin and acto-S-1 ATPase activities were inhibited appreciably by NA3 and NA4 (Figures 4–6). Actomyosin ATPase activities were inhibited by 30–50% ($p < 0.01$) at these concentrations, while NA3 and NA4 inhibited actin-activated S-1 ATPase activities by more than 90%

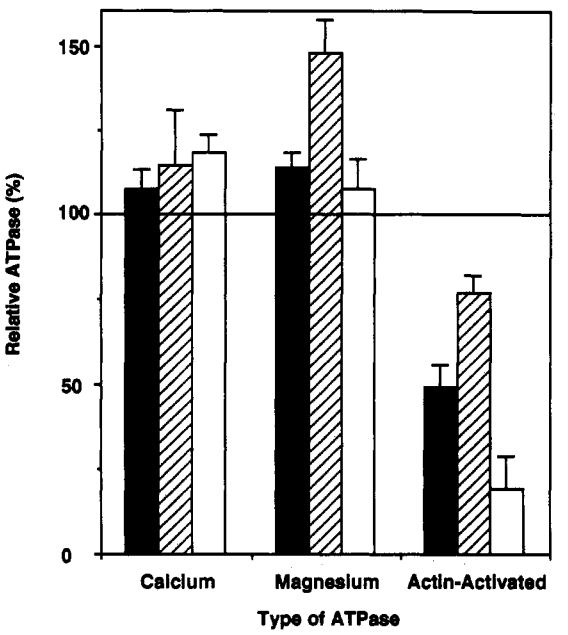

FIGURE 4: Effect of nebulin fragments on the ATPase activities of myosin, S-1, and acto-S-1. ATPase activities of myosin (0.25 μM) or chymotryptic S-1 (0.5 μM) were measured in the presence and absence of 1 μM NA4 or 2 μM NA3. The calcium ATPase was measured in 50 mM KCl, 5 mM $CaCl_2$, and 2 mM Tris (pH 7.4). The magnesium and actin-activated ATPases were measured in 4 mM $MgCl_2$, 1 mM $CaCl_2$, and 25 mM imidazole (pH 7.0), plus 25 mM KCl for myosin or 2 mM KCl for S-1. Actin-activated ATPase activities were assayed with 1 μM actin, and the basal magnesium ATPase activity (0.084 s^{-1}) was subtracted out. The phosphate release from ATP (2 mM) at 25 °C was determined by the malachite green assay (Baykov et al., 1988). Solid bar: NA3 and myosin ATPase activities. Hatched bar: NA4 and myosin ATPase activities. Open bar: NA4 and S-1 ATPase activities. Bars indicate the standard error of the mean for at least five determinations. Control ATPase activities were as follows: calcium ATPase, 2.7 ± 0.2 s^{-1} myosin and 3.4 ± 0.2 s^{-1} S-1; magnesium ATPase, 0.06 ± 0.01 s^{-1} myosin and 0.06 ± 0.01 s^{-1} S-1; and actin-activated ATPase, 0.88 ± 0.04 s^{-1} myosin and 0.96 ± 0.06 s^{-1} S-1.

(Figures 4–6). Under similar conditions, neither fragment inhibited the basal magnesium ATPase activity of S-1 alone (Figure 4).

To gain further insight into the mechanism by which NA3 inhibits acto-S-1 ATPase activity, binding studies were performed under ATPase assay buffer conditions. ELISA was used to determine dissociation constants for the interactions of solid-phase NA3 with actin (K_d = 1.2 ± 0.2 μM) and S-1 (K_d = 0.3 ± 0.1 μM). The dissociation constant for actin binding to NA3 was confirmed by a cosedimentation assay (K_d = 1.1 ± 0.2 μM). To determine whether actin and S-1 competed for binding to NA3, the effects of varying concentrations of actin (0–7.2 μM) on the binding of S-1 (0.5 μM) to solid-phase NA3 were measured by ELISA (Figure 5, inset). The presence of ATP in the binding buffer dissociates nearly all of the S-1 from actin under these conditions (Chalovich & Eisenberg, 1982), and a monoclonal antibody specific for S-1 was used to detect the NA3–S-1 complex. The data show that actin did not compete with S-1 for binding to solid-phase NA3. NA3, thus, contains distinct binding sites for both actin and S-1 and is capable of forming actin–nebulin–myosin complexes (Figure 5, inset).

Given these binding characteristics, it was possible to begin to evaluate whether the binding of NA3 to actin and/or S-1 was involved in the inhibition of acto-S-1 ATPase activity. For this purpose, actin-activated S-1 ATPase activity with 0, 2, and 10 μM NA3 was studied over a range of actin

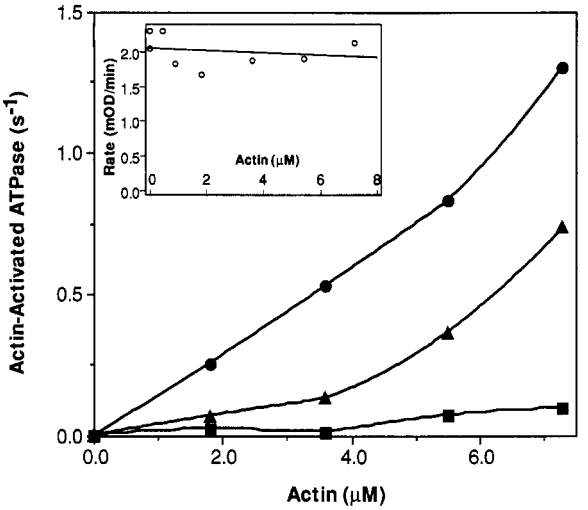

FIGURE 5: Effect of varying concentrations of NA3 on actin-activated S-1 ATPase activities. The ATPase activities of chymotryptic S-1 (0.5 μM) were measured in the absence (●) and presence of 2 μM NA3 (▲) or 10 μM NA3 (■) and various concentrations of actin (0–7.2 μM) in a buffer containing 2 mM KCl, 2 mM $MgCl_2$, 1 mM $CaCl_2$, and 10 mM imidazole (pH 7.0). The phosphate release from ATP (2 mM) at 25 °C was determined by the malachite green assay (Baykov et al., 1988). The background magnesium ATPase activity of S-1 alone was subtracted out. The curves were fit by interpolation. Inset: NA3 binding to S-1 in the presence and absence of actin. NA3 was adsorbed to the microtiter plate, blocked with BSA, and incubated with 0.5 μM S-1 in the presence of varying concentrations of actin (0–7.2 μM). Bound S-1 was detected by ELISA. The data are fit by linear regression. Buffer conditions are the same in ATPase and binding assays.

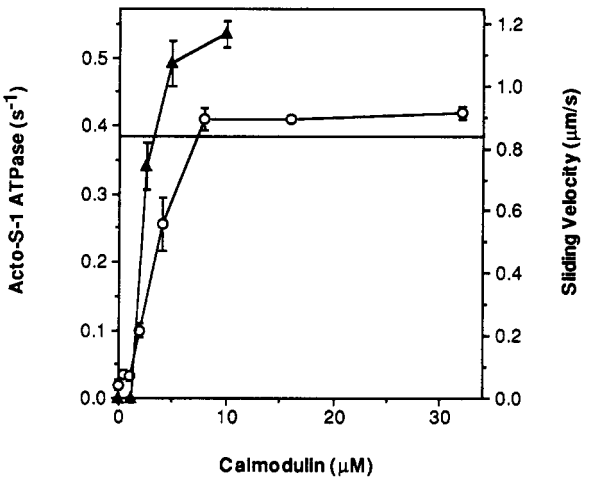

FIGURE 6: Calmodulin reverses the inhibition by NA4 of ATPase activities and actin sliding velocities. The inhibition by NA4 (1.7 μM) of actin-activated S-1 ATPase activities (○, 1 μM actin, 0.5 μM S-1) was assayed in the presence of increasing concentrations of calmodulin. The *in vitro* motility assays (▲) were performed using 1 μM NA4 (as in Figure 8). The horizontal line represents actin sliding velocities (0.84 ± 0.04 μm/s) and ATPase activities in the absence of NA4 (0.38 ± 0.02 s^{-1}). All curves are fit by interpolation. Bars indicate the standard error of the mean.

concentrations (0–7.2 μM) (Figure 5, with the basal S-1 magnesium ATPase activity subtracted out). In the absence of NA3, the ATPase activity increases linearly with the actin concentration. At 2 μM NA3, the ATPase activity curve is concave upward, approaching the value in the absence of NA3 at higher actin concentrations. At 10 μM NA3, the actin-activated S-1 ATPase activity is almost completely inhibited. Since the S-1 (0.5 μM) and actin concentrations (0–7.2 μM) used are well below the K_d of acto-S-1 binding in the presence of ATP [50–500 μM: Chalovich and Eisenberg (1982) and Root and Reisler (1992) or K_m = 20 μM: Root and Reisler (1991) and Cook et al. (1993)], the acto-S-1 complex and ATPase activity will increase approximately linearly with the concentration of actin, as described by the following equation:

$$A = [\text{actin–S-1}]k$$

where A is the actin-activated ATPase and k is a constant that depends on V_{max} and the efficiency with which actin activates S-1 ATPase.

In the presence of NA3, the acto-S-1 ATPase activity was dependent on the concentrations of both actin and NA3 (Figure 5). The following species may be present under these conditions: [S-1], [actin], [NA3], [actin–S-1], [NA3–S-1], [NA3–actin], [S-1–NA3–actin], [NA3–S-1–actin], [NA3–actin–S-1], and [S-1–NA3–actin]. If we assumed that the binding of NA3 to actin did not play a role in the effect of NA3 on acto-S-1 ATPase, and that the binding of NA3 to S-1 completely blocked actin-activated ATPase activity, the following equation would describe the ATPase activity in the presence of NA3:

$$A = ([\text{actin–S-1}] + [\text{NA3–actin–S-1}])k$$

The actin-activated ATPase would be predicted to increase approximately linearly with actin concentration. In contrast to this prediction, the ATPase activities in the presence of 2 μM NA3 do not increase linearly with actin concentration (Figure 5). Using the dissociation constant of NA3 binding to S-1 of 0.3 ± 0.1 μM (determined by ELISA as described above), and assuming a stoichiometry of two S-1 per NA3 (n = 0.5) as estimated from NA3 cosedimentation assays with myosin, it can be calculated from the binding equation (cf. Experimental Procedures)

$$\% \text{ S-1 bound by NA3} = 100[nP + K_d + N - \sqrt{(nP + K_d + N)^2 - 4nPN}]/2nP$$

that the percentage of S-1 (0.5 μM = P) that binds NA3 (N) is 87% at 2 μM NA3. This value is much higher than the percentage of inhibition of ATPase activity at 2 μM NA3 at high actin concentrations. Therefore, the binding of NA3 to S-1 alone cannot explain the inhibition of acto-S-1 ATPase activity, and the binding of NA3 to actin must play some role in the inhibition of acto-S-1 ATPase activity.

The actin-activated ATPase activities could be restored completely by the addition of calmodulin in the presence of calcium (Figure 6). Nebulin fragment NA4 (1.7 μM) inhibited acto-S-1 ATPase activity (1 μM actin and 0.5 μM S-1) in the presence of calcium (1 mM). The addition of increasing concentrations (to 30 μM) of calmodulin caused a release of inhibition, with a half-maximum dose of 4 μM calmodulin (Figure 6). Beyond 10 μM calmodulin, the acto-S-1 ATPase was slightly activated.

Effect of Nebulin on Actin Sliding over Myosin in Motility Assays. The inhibitory effect of the nebulin fragment on actomyosin ATPase led us to investigate its effects on the mechanical properties of the sliding velocity of actin over myosin by *in vitro* motility assays. The sliding velocity of rhodamine phalloidin-labeled actin over heavy meromyosin on a nitrocellulose-coated coverslip at 20 °C was studied in the presence of various concentrations of five nebulin fragments (NA4, NA3, NC17, ND66, and ND8) and of calmodulin (10 μM) and calcium (0.1 mM). In the assay buffer at 20 °C, the actin filaments slide with a mean velocity of 0.91 ± 0.17

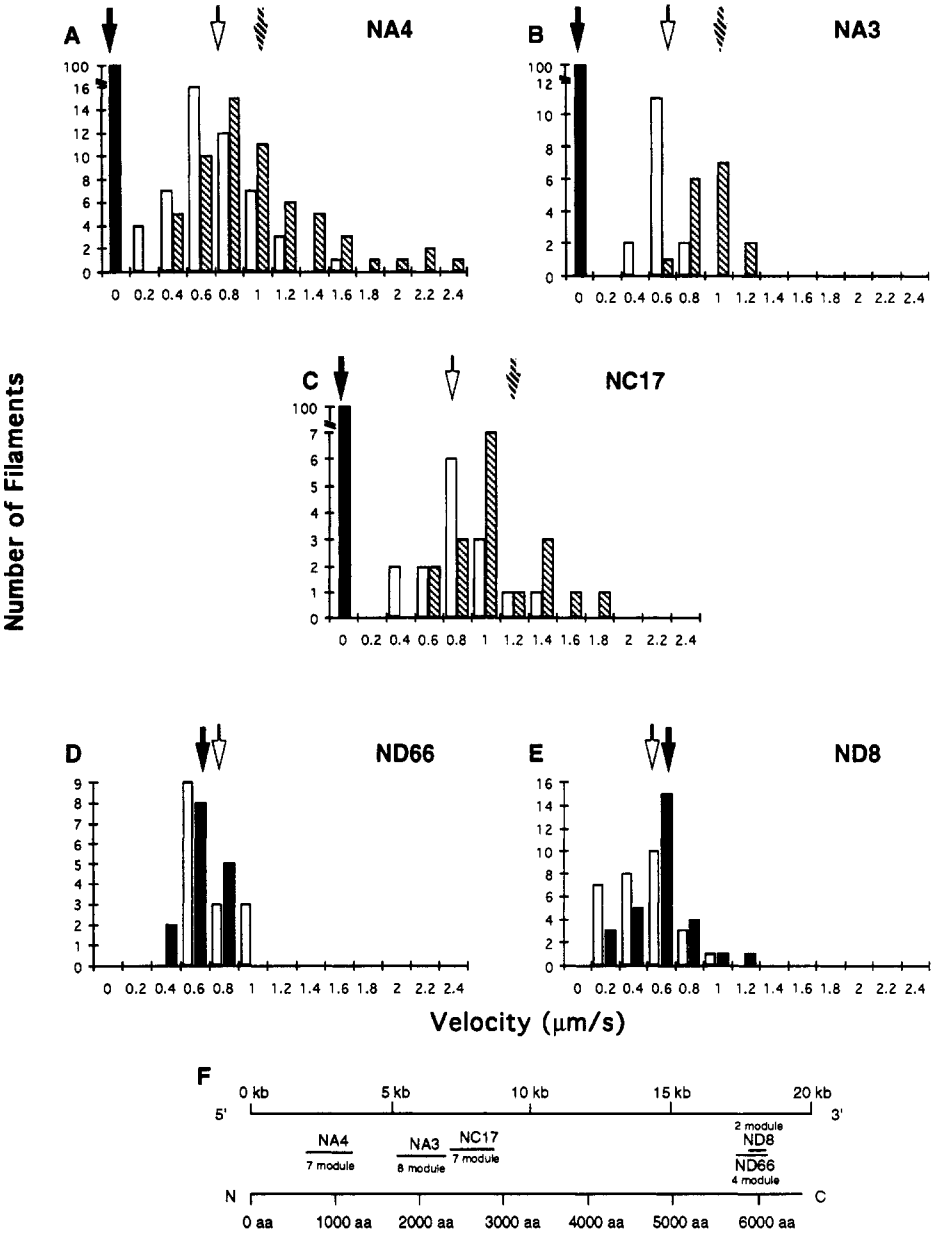

FIGURE 7: Nebulin–calmodulin regulation of actin sliding. Velocity distribution histograms of actin sliding (open bars and arrows) and in the presence of nebulin fragment (solid bars and arrows) and nebulin fragment plus calmodulin (10 μM) and calcium (striped bars and arrows). Conditions are as described in Table 2. Mean velocities are indicated by the arrows for the following nebulin fragments: (A) NA4, 0.5 μM; (B) NA3, 0.7 μM; (C) NC17, 0.9 μM; (D) ND66, 40 μM; (E) ND8, 400 μM. The addition of calmodulin was not attempted for ND66 and ND8. (F) The relative sizes and positions of the different nebulin fragments along the sequenced human nebulin molecule. The unsequenced middle portion of nebulin is indicated by hatch marks at about 3000 amino acids (aa).

μm/s. The addition of calmodulin alone at pCa = 4.0 caused no significant change in the sliding velocity (Table 2). Two types of behavior were observed in the presence of a nebulin fragment. The group of three fragments NA4, NA3, and NC17 (0.9 μM) completely inhibited actin sliding over skeletal muscle HMM in a 25 mM KCl motility buffer (Table 2). Although the dose–response curves of various nebulin fragments differ somewhat, complete inhibition occurred between 0.5 and 0.9 μM, and half-inhibition of the mean sliding velocity occurred between 0.3 and 0.5 μM, with NA4 being the most potent inhibitor of these fragments. These dose responses indicate a more graded inhibition of actin sliding similar to that of caldesmon, but do not display the all or none effects of calponin on actin sliding (Shirinsky et al., 1992). Even at salt concentrations approaching the maximum tolerated by the motility assay (80 mM KCl), NA3, NC17, and NA4 still inhibited actin sliding by 40–50% at 1 μM (data not shown). In contrast, a four-module fragment, ND66, that overlaps with ND8 near the Z-line (Huang, 1993; Wright et al., 1993) showed at best only marginal inhibition of actin sliding (Table 2). ND66 (40 μM) caused the actin sliding velocity to decrease from 0.84 ± 0.04 to 0.74 ± 0.03 μm/s (SE) in the standard motility assay buffer.

Actin sliding was completely restored by the addition of calcium and calmodulin (Table 2 and Figures 6 and 7–9). The dose response of actin sliding in the presence of NA4 to calmodulin is similar to that in the ATPase assays (Figure 6). As shown in the sliding velocity distribution histograms of each of the five nebulin fragments (Figure 7), the complete inhibition by NA4, NA3, or NC17 (solid bars) was reversed by calmodulin. Indeed, the treatment appears to activate sliding significantly beyond the control velocities (Table 2, Figure 7). Some individual filaments slide at up to 3 times the control velocity (2.4 μm/s) in the presence of NA4 and CaM at pCa = 4. Calmodulin in the absence of nebulin

Table 2: Effect of Nebulin Fragments on Actin Sliding Velocity[a]

nebulin fragment (modules)	concentration (μM) for 50% inhibition	concentration (μM) for 100% inhibition	relative velocity with calmodulin[b] (%)
NA4 (7)	0.3	0.5	139
NA3 (8)	0.5	0.7	155
NC17 (7)	0.5	0.9	149
no nebulin	NA[c]	NA	92
ND66 (4)	NI[d]	NI	NI

[a] The sliding velocities of rhodamine phalloidin-labeled actin over chymotryptic heavy meromyosin on a nitrocellulose-coated coverslip were observed at 20 °C. Means for control actin sliding velocities averaged 0.91 ± 0.17 (SD) μm/s. Test measurements were compared to control values from the same coverslip. [b] Measured in the presence of 10 μM calmodulin and enough of each nebulin fragment to completely inhibit actin sliding. The 95% confidence limits for these values were <14%. Two-tailed t-tests indicated significant differences, $p < 0.02$, except for the no nebulin control. [c] NA, not applicable. [d] NI, no significant inhibition up to 40 μM ND66.

fragments did not accelerate actin sliding velocities (Table 2).

The presence of troponin and tropomyosin did not affect the ability of equimolar NA4 to inhibit actin sliding (in the presence of calcium and without calmodulin) or the subsequent reversal of this inhibition by calcium and calmodulin (Figure 9). Our reconstituted troponin–tropomyosin complex alone reversibly inhibited actin sliding over myosin in a calcium-dependent manner (Figure 9C), confirming its activity (Honda & Asakura, 1989). Calcium alone caused no reversal, indicating that the calcium effect is mediated through calmodulin or a calmodulin–nebulin complex.

The calcium dependence of the NA4–calmodulin system is illustrated in the leading edge plots and velocity distribution histograms in Figure 8, where actin sliding was studied on the same myosin-coated coverslip by sequentially varying the pCa to 4.0, 5.2, 6.4, 6.8, and back to 4.0. As shown in Figure 8A–F, where the leading edges of each sliding actin filaments were plotted over an 8 s span, sliding velocities remained constant between pCa = 4 and 6.4 and halted abruptly at pCa = 6.8. Raising the Ca^{2+} to pCa = 4.0 restored the slightly activated mean velocity (cf. Figure 8B,F).

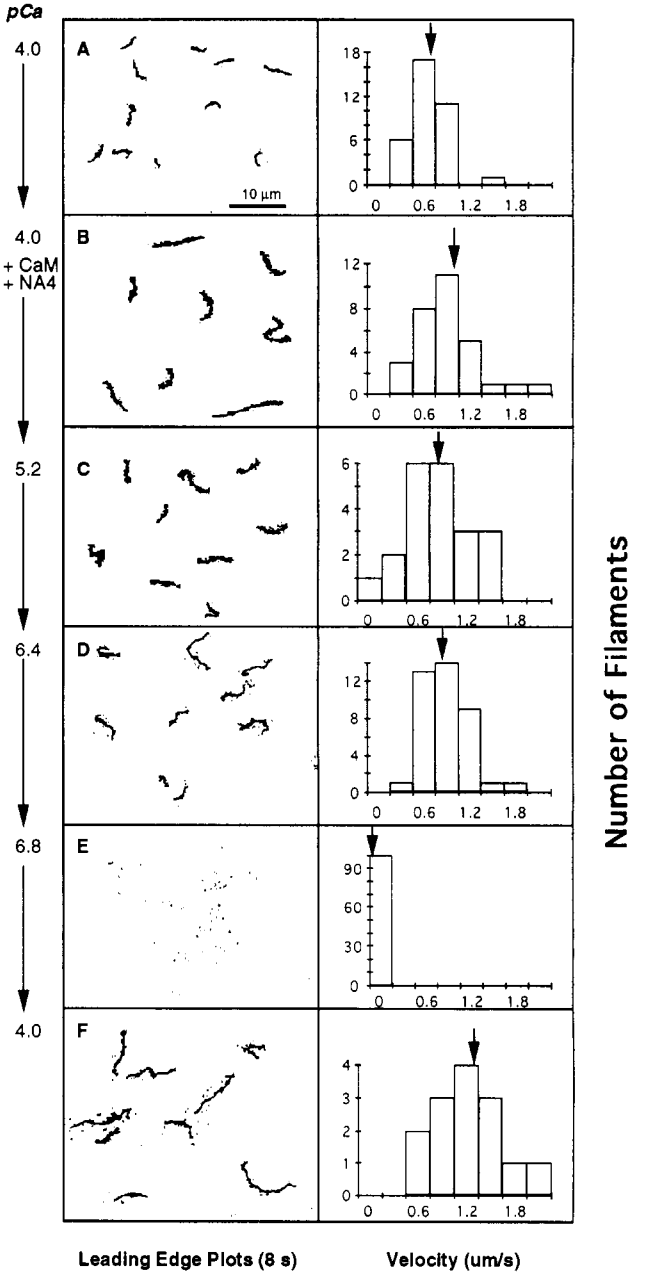

FIGURE 8: Calcium dependence of calmodulin–nebulin regulation of actin sliding. Leading edge plots of actin sliding over an 8 s time span and velocity distribution histograms are shown for a series of assays of actin sliding in the presence of NA4, calmodulin, and varying concentrations of free calcium. One coverslip was used for this entire experiment. Buffer conditions are as described in Table 2. The means of actin sliding velocities for all measured filaments (15–39 filaments per sample) are indicated by arrows. (A) pCa = 4.0, control actin filaments without calmodulin or NA4; (B) pCa = 4.0, 4 μM calmodulin, 0.6 μM NA4; (C) pCa = 5.2, 4 μM calmodulin, 0.6 μM NA4; (D) pCa = 6.4, 4 μM calmodulin, 0.6 μM NA4; (E) pCa = 6.8, 4 μM calmodulin, 0.6 μM NA4; (F) pCa = 4.0, 4 μM calmodulin, 0.6 μM NA4.

DISCUSSION

The protein interactions of cloned nebulin fragments reported here and elsewhere (Jin & Wang, 1991a,b; Kruger et al., 1991; Labeit et al., 1991; Chen et al., 1993) now provide structural insights and functional implications of the actin–nebulin composite thin filament of skeletal muscles. Our data for the nebulin fragments in the overlap region are consistent with a tentative working model depicted in Figure 10. In the model, the following features are assumed: (1) nebulin fragments bind alongside actin polymers; (2) nebulin fragments bind to myosin heads and juxtapose myosin heads to actin; (3) calmodulin binds to actin at a site(s) that is distinct from the actin and myosin sites; and (4) the presence of calcium induces conformational changes in nebulin that result in the dissociation of myosin heads and a loosening of actin binding, thereby allowing actomyosin interaction. For nebulin fragments near the Z-line (N66 and ND8), the binding to myosin appears weak or absent. These fragments, however, do bind to actin and calmodulin (Chen et al., 1993; G. Chen, C.-L. Shih, and K. Wang, unpublished data). Our data are discussed here in the context of these working hypotheses.

Nebulin as a Thin Filament Template. Our present study indicates that nebulin fragments containing a seven-module superrepeat bind with high affinity to the actin polymer. The apparent dissociation constants of these interactions are in the same range as those of troponin–tropomyosin and rigor binding of S-1 to actin (Mak et al., 1983). The binding of the entire nebulin molecule, which contains more than 20 of these superrepeats, therefore is likely to be much stronger than that of the individual fragments (Wang et al., 1990).

It is striking that, for both NA4 and NA3, there is unexpectedly only one, or no more than two, high-affinity binding sites in the submicromolar range. In view of the observations that a two-module fragment ND8 interacts with

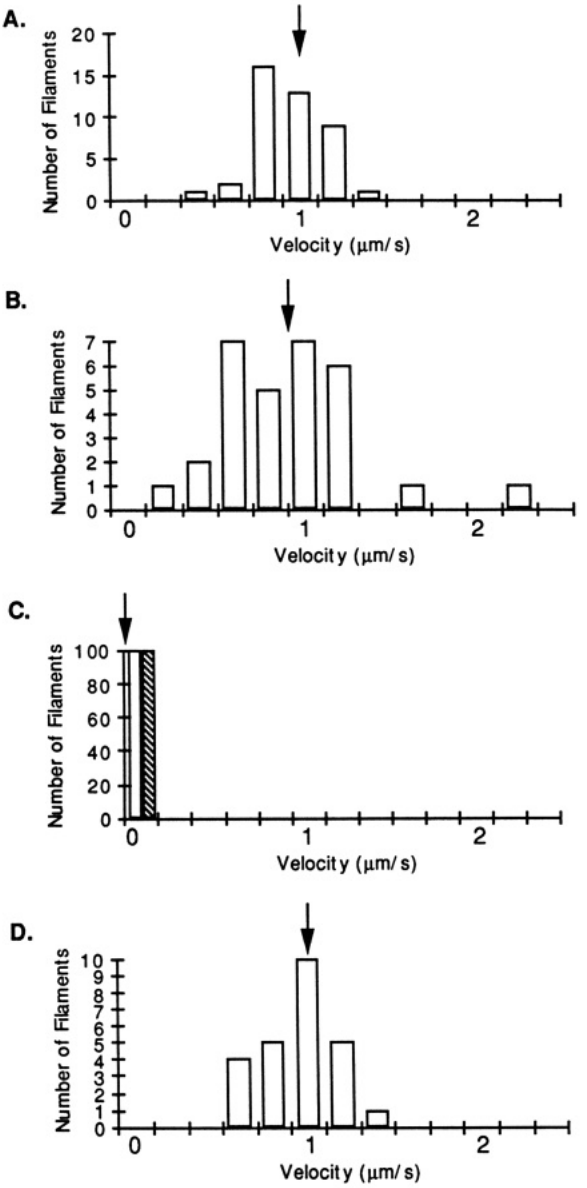

FIGURE 9: Nebulin–calmodulin regulation of actin sliding in the presence of troponin–tropomyosin. Velocity distribution histograms of actin sliding with sequentially added troponin–tropomyosin (B), NA4 (C), and calmodulin (D). Buffer conditions are as described in Table 2. Means of actin sliding velocities for all measured filaments are indicated by arrows for the following conditions: (A) actin and myosin alone; (B) troponin (1.5 μM), tropomyosin (1.5 μM), actin, and myosin; (C) troponin (1.5 μM), tropomyosin (1.5 μM), actin, myosin with (open bars) NA4 (1.5 μM) or with (striped bars) 5 mM EGTA in the absence of NA4; and (D) calmodulin (10 μM), NA4 (1.5 μM), troponin (1.5 μM), tropomyosin (1.5 μM), actin, and myosin.

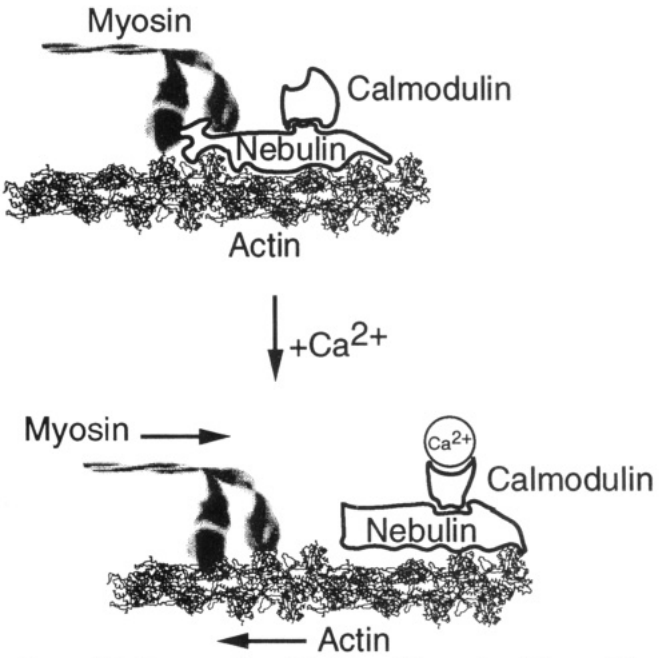

FIGURE 10: Conceptual model of the calcium–calmodulin-sensitive interaction of nebulin fragments with actin and myosin *in vitro*. A cartoon illustrating the calcium-sensitive interaction of a nebulin–calmodulin complex with actin and myosin. The stoichiometry of interaction and relative size and shape of nebulin and calmodulin are arbitrary. See text for details.

F-actin with low affinity [20–40 μM; see Chen et al. (1993)] and single-module sequences with even lower affinity [200–500 μM; see Pfuhl et al. (1994)], it is plausible that each of the seven types of modules of the superrepeat displays distinct intrinsic affinity toward actin, with one or two high-affinity types. Since these lower affinity modules would not be expected to compete effectively with the high-affinity sites for actin binding, especially at high nebulin concentrations, these sites may be difficult to detect under our assay conditions.

Immunolocalization studies (Wang & Wright, 1988; Pierobon-Bormioli et al., 1989; Maruyama et al., 1989; Jin & Wang, 1991a; Kruger et al., 1991; Wright et al., 1993), especially studies utilizing sequence-specific monoclonal antibodies (Wright et al., 1993), have indicated that one nebulin polypeptide extends the entire length of the thin filament and support the notions that each module spans the spacing of one actin protomer and that one superrepeat spans seven actin protomers or one thin filament repeat of 38–40 nm. Our binding data, if applicable *in situ*, suggest that nebulin polypeptides make only one tight contact for every seven actin molecules along the double helix, with the intervening modules making loose associations with actin protomers between the high-affinity sites. Such a variation in affinity between nebulin and actin may have functional implications, since these lower affinity modules may be more easily accessible to other nebulin binding proteins, such as myosin, C-protein, calmodulin (Patel et al., 1988), and α-actinin (Nave et al., 1990).

The binding study of myosin extends our earlier solid-phase assays (Jin & Wang, 1991a) and provides a clue to the multiple functionality of nebulin. The binding of NA4 and NA3 to myosin and S-1 with high affinity raises the possibility that, *in situ*, nebulin may cross-link or tether actin to myosin in rigor and the attachment is subsequently released when calcium binds to nebulin-associated calmodulin, e.g., during activation. It is significant that calmodulin did not, even at high concentrations, completely inhibit actin–nebulin binding (Figure 2A,C), suggesting a more tenacious association of nebulin with actin than myosin. The strong binding of calmodulin to nebulin in the presence and absence of calcium was also reported by Patel et al. (1988) by protein overlaying techniques. It is thus likely that calmodulin and nebulin may form a relatively stable complex that coexists with tropomyosin–troponin on the thin filaments of skeletal muscle.

Nebulin as a Regulatory Protein. The observation that nebulin fragments inhibited both actomyosin ATPase and actin sliding in motility assays provides, for the first time, strong evidence for a regulatory role for nebulin. Most interestingly, this inhibition is reversed by calmodulin in a calcium-dependent manner. The pCa required for reversal in the motility assay was found to be 6.4–6.8, corresponding closely to the pCa

levels that induce the contraction of skeletal muscle fibers.

In skeletal muscle, calmodulin is abundant and is present in the I bands where nebulin is also found (Sweeney et al., 1993; Harper & Steiner, 1983). Calmodulin may mediate the effect of calcium on nebulin *in situ*. Alternatively, in view of the homology between troponin C and calmodulin (Jamieson et al., 1980), it is possible that troponin C might interact with nebulin and mediate calcium regulation. However, we found that troponin complex at concentrations of up to 5 μM and pCa = 4 did not reverse the inhibition of acto-S-1 ATPase activity by NA4 (not shown).

It is significant that NA4 and NA3 inhibit actin sliding at concentrations corresponding to the apparent dissociation constant of binding to actin (cf. Tables 1 and 2), suggesting that actin binding may contribute to the inhibition. It is conceivable that the tethering or cross-linking of actin to myosin by nebulin may inhibit actin sliding. Additionally, its inhibitory effect on ATPase activity may also contribute to the inhibition. Nebulin, being a basic protein (Wang et al., 1990; Jin & Wang, 1991a), might compete with myosin for interaction with the acidic amino terminus of actin at the actomyosin interface (Rayment et al., 1993). To our knowledge, nebulin is the only protein found to increase actin sliding over skeletal muscle myosin. Tropomyosin (Umemoto et al., 1989; Umemoto & Sellers, 1990; Okagaki et al., 1991) and *Physarium* caldesmon-like protein (Ishikawa et al., 1991) are reported to accelerate actin sliding over smooth muscle myosin but not skeletal muscle myosin. Smooth muscle caldesmon has been proposed to tether actin and myosin together in smooth muscle (Haberle et al., 1992). Striking parallels between nebulin and caldesmon exist: (1) both are capable of linking actin and myosin, which can aid or inhibit actin sliding in motility assays; (2) both are able to inhibit actin-activated ATPase activity; and (3) both can be modulated by calmodulin and calcium (Walsh, 1990; Shirinsky et al., 1992). It is an intriguing idea that nebulin might perform some of the functions in skeletal muscle that caldesmon does in smooth muscle.

A group of nebulin fragments NA3, NA4, and NC17, which constitute a total of four of the more than 20 superrepeats, display similar regulated inhibitory effects in motility assays. These fragments are localized near the N-terminal side of nebulin, which normally overlaps with myosin filaments in the sarcomere. It should be pointed out that we also observed that a four-module fragment ND66 (which contains the ND8 sequence; Jin & Wang, 1991a; Chen et al., 1993) near the C-terminus of nebulin did not significantly inhibit actin sliding. It is conceivable that these modules do not contain the sequences necessary for this function or that a minimal number of six modules is required for the regulatory function. Since ND66 is at or near the Z-line (Wright et al., 1993) and is out of the normal reach of myosin filaments, such a function may not be necessary. ND66 appears to be a useful control to rule out the possibility that the basic charge alone is sufficient for this regulatory function of nebulin modules.

Nebulin–Calmodulin as a Candidate for a New Calcium Regulatory Pathway. In skeletal muscle, regulations by myosin light-chain kinase, which potentiates posttetanic twitch tension (Sweeney et al., 1993), and by tropomyosin–troponin, which turns on and off thin filaments, have been well characterized (Zot & Potter, 1987). Our data suggest the nebulin–calmodulin system is a candidate for a new thin-filament-based regulatory pathway that is distinct from the troponin–tropomyosin pathway. Nebulin might regulate the mechanical coupling between myosin motors and the sliding velocity of actin filaments. Indeed, the protein interactions in solution among nebulin, calmodulin, actin, and myosin are highly reminiscent of the behavior of smooth muscle caldesmon (Walsh, 1990). By analogy, it is conceivable that nebulin filaments *in situ* may juxtapose myosin heads to the actin filaments and help orient myosin motors for maximal and efficient interaction with actin. Nebulin's ability to bind both actin and myosin may indicate a structural role for nebulin in maintaining the proper alignment of myosin filaments in the sarcomere, thus acting as a zipper to hold thin and thick filaments together at proper lattice spacing.

ACKNOWLEDGMENT

We thank Dr. Alan Brady for his critical review of the manuscript and Dr. James Lin for donating the JLA20 anti-actin monoclonal antibodies.

REFERENCES

Baykov, A. A., Evtushenko, O. A., & Avaeva, S. M. (1988) *Anal. Biochem. 171*, 266–270.
Chalovich, J. M., & Eisenberg, E. (1982) *J. Biol. Chem. 257*, 2432–2437.
Chen, M. G., & Wang, K. (1993) *Arch. Biochem. Biophys.*, in press.
Chen, M. G., Shih, C. L., & Wang, K. (1993) *J. Biol. Chem. 268*, 20327–20334.
Cook, R. K., Root, D., Miller, C., Reisler, E., & Rubinstein, P. A. (1993) *J. Biol. Chem. 268*, 2410–2415.
Cummins, P., & Perry, S. V. (1973) *Biochem. J. 133*, 765–777.
Eisenberg, E., & Kielley, W. W. (1974) *J. Biol. Chem. 249*, 4742–4748.
Fabiato, A. (1988) *Methods Enzymol. 157*, 378–417.
Gill, S. C., & von Hippel, P. H. (1989) *Anal. Biochem. 182*, 319–326.
Godfrey, J., & Harrington, W. F. (1970) *Biochemistry 9*, 886–895.
Gottlieb, M., & Chavoko, M. (1987) *Anal. Biochem. 165*, 33–37.
Haeberle, J. R., Trybus, K. M., Hemric, M. E., & Warshaw, D. M. (1992) *J. Biol. Chem. 267*, 23001–23006.
Harper, J. F., & Steiner, A. L. (1983) *Methods Enzymol. 102*, 122–143.
Hartshorne, D. J. (1987) *Physiology of the Gastrointestinal Tract* (Johnson, L. R., Ed.) pp 423–482, Raven Press, New York.
Homsher, E., Wang, F., & Sellers, J. (1992) *Am. J. Physiol. 262*, C714–C723.
Honda, M., & Asakura, S. (1989) *J. Mol. Biol. 205*, 677–683.
Huang, J.-P., Tang, C.-J. C., Kou, G.-H., Marchesi, V. T., Benz, E. J. J., & Tang, T. K. (1993) *J. Biol. Chem. 268*, 3758–3766.
Ishikawa, R., Okagaki, T., Higashi-Fujime, S., & Kohama, K. (1991) *J. Biol. Chem. 266*, 21784–21790.
Jamieson, G. A., Jr., Bronson, D. D., Schachat, F. H., & Vanaman, T. C. (1980) *Ann. N.Y. Acad. Sci. 356*, 1–13.
Jin, J.-P., & Wang, K. (1991a) *J. Biol. Chem. 266*, 21215–21223.
Jin, J.-P., & Wang, K. (1991b) *FEBS Lett. 281*, 93–96.
Kielley, W. W., & Bradley, L. B. (1956) *J. Biol. Chem. 218*, 653–659.
Kron, S. J., Toyoshima, Y. Y., Uyeda, T. Q. P., & Spudich, J. A. (1991) *Methods Enzymol. 196*, 399–416.
Kruger, M., Wright, J., & Wang, K. (1991) *J. Cell Biol. 115*, 97–107.
Labeit, S., Gibson, T., Lakey, A., Leonard, K., Zeviani, M., Knight, P., Wardale, J., & Trinick, J. (1991) *FEBS Lett. 282*, 313–316.
Laemmli, U. K. (1970) *Nature 227*, 680–685.
Lin, J. J.-C. (1981) *Proc. Natl. Acad. Sci. U.S.A. 78*, 2335–2339.
Mak, A. S., Golosinska, K., & Smillie, L. B. (1983) *J. Biol. Chem. 258*, 14330–14334.

Maruyama, K., Matsuno, A., Higuchi, H., Shimaoka, S., Kimura, S., & Shimizu, T. (1989) *J. Muscle Res. Cell Motil. 10*, 350–359.
Miller, J. B., Teal, S. B., & Stockdale, F. E. (1989) *J. Biol. Chem. 264*, 13122–13130.
Nave, R., Fürst, D. O., & Weber, K. (1990) *FEBS Lett. 269*, 163–166.
Okagaki, T., Higashi-Fujime, S., Ishikawa, R., Takano-Ohmuro, H., & Kohama, K. (1991) *J. Biochem. (Tokyo) 109*, 858–866.
Patel, K., Strong, P. N., Dubowitz, V., & Dunn, M. J. (1988) *FEBS Lett. 234*, 267–271.
Pfuhl, M., Winder, S. J., & Pastore, A. (1994) *EMBO J. 13*, 1782–1789.
Pierobon-Bormioli, S., Betto, R., & Salviati, G. (1989) *J. Muscle Res. Cell Motil. 10*, 446–456.
Potter, J. D. (1982) *Methods Enzymol. 85*, 241–263.
Rayment, I., Holden, H. M., Whittaker, M., Yohn, C. B., Lorenz, M., Holmes, K. C., & Milligan, R. A. (1993) *Science 261*, 58–65.
Root, D. D., & Reisler, E. (1990) *Anal. Biochem. 186*, 69–73.
Root, D. D., & Reisler, E. (1992) *Biophys. J. 63*, 730–740.
Root, D. D., & Wang, K. (1993) *Anal. Biochem. 209*, 15–19.
Root, D. D., Cheung, P., & Reisler, E. (1991) *Biochemistry 30*, 287–294.
Shirinsky, V. P., Biryukov, K. G., Hettasch, J. M., & Sellers, J. R. (1992) *J. Biol. Chem. 267*, 15886–15892.
Smillie, L. B. (1982) *Methods Enzymol. 85*, 234–241.
Spudich, J. A., & Watt, S. (1971) *J. Biol. Chem. 246*, 4866–4871.
Stedman, H., Browning, K., Oliver, N., Oronzi-Scott, M., Fischbeck, K., Sarkar, S., Sylvester, J., Schmickel, R., & Wang, K. (1988) *Genomics 2*, 1–7.
Sweeney, H. L., Bowman, B. F., & Stull, J. T. (1993) *Am. J. Physiol. 264*, C1085–C1095.
Umemoto, S., & Sellers, J. R. (1990) *J. Biol. Chem. 265*, 14864–14869.
Umemoto, S., Bengur, A. R., & Sellers, J. R. (1989) *J. Biol. Chem. 264*, 1431–1436.
Walsh, M. P. (1990) *Biochem. Cell Biol. 69*, 771–800.
Wang, K. (1985) *Cell and Muscle Motility* (Shay, J. W., Eds.) Vol. 6, pp 315–369, Plenum Publishing Corporation, New York.
Wang, K., & Wright, J. (1988) *J. Cell Biol. 107*, 2199–2212.
Wang, K., Knipfer, M., Huang, Q. Q., Hsu, L., van Heerden, A., Browning, K., Quian, X., & Stedman, H. (1990) *J. Cell Biol. 111*, 428a.
Weeds, A., & Pope, B. (1977) *J. Mol. Biol. 111*, 129–157.
West, J. J., Nagy, B., & Gergely, J. (1967) *J. Biol. Chem. 242*, 1140–1145.
Wright, J., Huang, Q., & Wang, K. (1993) *J. Muscle Res. Cell Motil. 14*, 476–483.
Young, D. M., Himmelfarb, S., & Harrington, W. F. (1965) *J. Biol. Chem. 240*, 2428–2436.
Zot, A. S., & Potter, J. D. (1987) *Annu. Rev. Biophys. Biophys. Chem. 16*, 535–559.